Structural and optical properties of CdS/PVA nanocomposites thin films

Furqan A. Kasim

Department of Physics/ College of Science/ University of Basrah/ Basrah/ Iraq.

furqan_kasim@yahoo.com

Abstract

CdS nanoparticles are successfully capped by poly vinyl-alcohol (PVA). In additional, CdS/PVA nanocomposites thin films were synthesized using chemical bath deposition method on microscopic glass substrates at 75 ^{o}C. Cadmium acetate $Cd(CH_3OOH)_2$ and cadmium chloride ($CdCl_2$) were used as a cadmium (Cd^{2+}) ions source while thiourea was used as a sulphur ions (S^{2-}) source with different molar concentrations of PVA. The structural properties of the obtained samples were characterized using X-ray diffraction technique (XRD). The variation of the polymer molar concentrations on the structural parameters such as the lattice constants, the strain value and the dislocation density has been obtained. The Fourier transform infrared spectra (FTIR) of pure PVA, CdS powder and PVA capped CdS nanoparticles was studied and the vibration bands were determined. The transmission electron microscopy (TEM) images of one of samples showed the bonding of the CdS-PVA nanocomposites. The optical absorption spectra of the CdS/PVA nanocomposites thin films were studied and the values of optical energy gap of the nanocomposites thin films have been calculated. The particles size of CdS nanoparticles and CdS/PVA nanocomposites that were calculated from the X- ray data and the optical band gap are affected by the PVA molar concentrations.

Keywords: CdS, PVA, Chemical Bath Deposition, XRD, FTIR,Optical energy gap.

Introduction

The synthesis and characterization of semiconductor nanoparticles have recently gained tremendous attention owing to their unique chemical and physical properties beside the huge potential for practical application of the composite system incorporating the nanoparticles [H.F Al-Taay et al. 2013 and M.A. Mahdi et al. 2012]. These properties differ significantly from those of the bulk material, which is related to the quantum size effect and the high surface to volume effects [H. Zhao et al**.** 2001, H.F Al-Taay et al. 2013 and M.A. Mahdi *et al.* 2012]. Furthermore, many atoms become a part of the crystallite surface when the particles size approach to nanosize compared to bulk atoms. These surface atoms are not fully bonded with the crystal backbone, which make them highly reacting with the environment to exhibit another unusual physical or chemical phenomena [J. Kuljanin *et al*. 2006 and M.A Mahdi *et al*. 2012]. In the other hand, semiconductor nanoparticles are highly unstable, and without trapping media, they coalesce quickly. For this reason, bonding of capping agents to nanoparticles is essential to yield chemical passivation, as well as to enhance the surface state which has a serious influence on the optoelectronics properties of nanoparticals and made a control of the growth of nanoparticals [S.H. Liu *et al***.** 2002, I.S. Elashamawi *et al*. 2009]. Via carefully controlling the size and surface structure of semiconductor materials, the electronics, optical, magnetic, mechanical, and chemical properties can be adjusted to matching a vast range of device application in numerous fields [H. Zhao *et al*. 2001]. As a result, the polymer matrix has been frequently used to produce semiconductor-polymer nanocomposites. The polymer host matrix plays to confine the growth of nanoparticles and prevents aggregation. Many applications of nanoparticles need stable and rigid forms, such as thin films. The Usage of polymer as the matrix for nanoparticle additions enables easy fabrication of nanocomposites films [J. D. Patela *et al*. 2009, M**.** Pattabi et al. 2007]. The semiconductor cadmium sulfide (CdS) material with 2.42eV direct energy gap at room temperature, and its optical and electrical properties made CdS suitable to be used in the manufacture of various devices such as solar cells, light-emitting diodes,

catalysts and other optoelectronic devices [W. Qingqing et al. 2005, R.Maity and K.K. Chattopadhyay 2006, Y.C. Zhang *et al.* 2007].The literature carries many reports on synthesis and characterization of CdS/PVA nanocomposites thin films and PVA capped CdS nanoparticles by using different methods. In this study, we synthesis CdS/PVA nanocomposites thin films and PVA capped CdS nanoparticles with two different cadmium ions sources, and the structural and optical properties of prepared samples were investigated**.**

2. Experimental

2.1 Samples Preparation

All chemicals used were of analytical grade and without further purification. CdS nanostructure and CdS/PVA nanocomposites were synthesized using two cadmium sources. Firstly, to prepare CdS nanostructure: cadmium acetate ($Cd(CH_3OOH)_2$ and cadmium chloride ($CdCl_2$) as follows: two sets of 0.1M aqueous solution of cadmium acetate and cadmium chloride are mixed with 0.1M aqueous solution of thiourea using magnetic stirrer. Then, 1M aqueous solution of ammonium acetate was added to the mixture with drop wise of diluted ammonia (NH_3) solution to raising the pH to 10. Finally, very well cleaning microscopic glass substrates were inserted in the beaker contained the above solution at temperature of 80^{o}C for 2 hours. To synthesis of CdS/PVA nanocomposites thin films: PVA powder was dissolved by 100ml of distillate water and the resulting solution was gently mixed at a temperature of 75^{o}C for 30 min. Then, the same solution, which used to prepare CdS nanostructure, was added to the PVA solution except the thiourea was drop wise added in the final step to the mixture. Finally, well cleaned glass substrates were inserted vertically in the beaker contained the prepared solution. After 30 min, the color of the solution was changed to bright yellow indicating the formation of CdS. Thin films of CdS-PVA nanocomposites was deposited on the glass substrate. At the end of the reaction, the solution was a yellow translucent colloidal solution, which was stored to stable at room temperature for seven days. After centrifugation with a speed of 3000 rpm, the products was washed with distilled water several times and then

dried. CdS nanoparticles were prepared by changing the amount of PVA (1g and 1.5g) and the concentration of cadmium acetate was fixed at 0.1M. Table1 contained the details of the prepared samples.

Figure 1 shows schematic of the reaction mechanism of the Cd^{++} ions combines with the PVA monomers by bonding with the hydroxyl. Then, after addition of thiourea the S^{--} ions will bond with the Cd^{++} to create CdS nanoparticles.

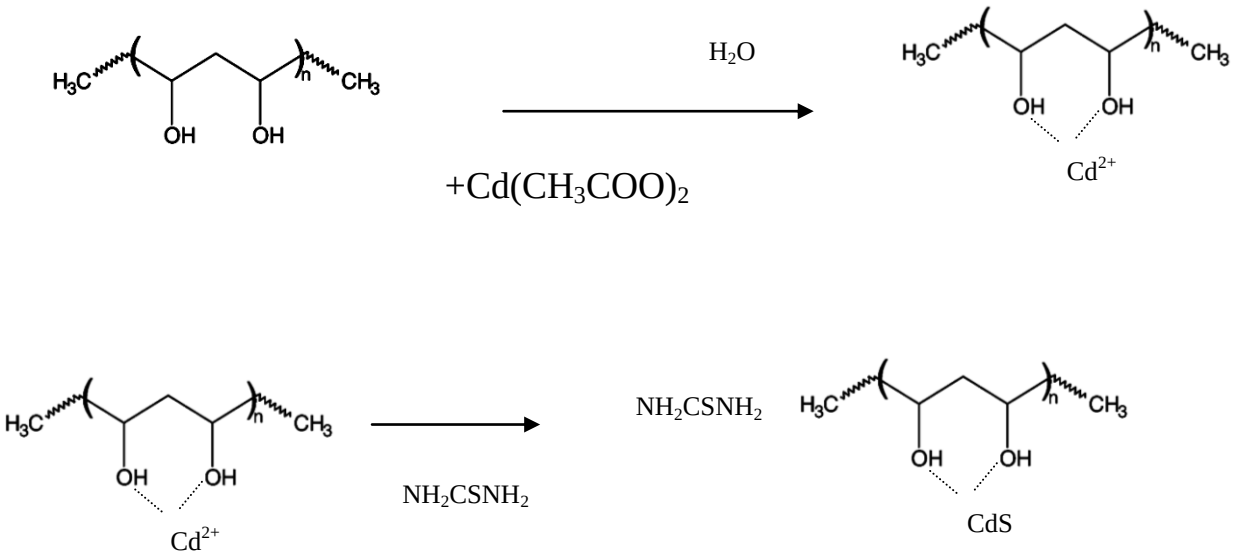

Fig.1: Schematic of the reaction of CdS/PVA nanocomposites.

Table (1): The preparation conditions of the samples.

Sample	**Cd^{2+} source**	**Molarities of Cd^{2+} source and thiouria**	**PVA (wt.)grm**	**Case**
S_1	-	-	0.1	PVA pure
S_2	CdAc.	0.1	0	CdS powder
S_3	$CdCl_2$	0.1	0	CdS powder
S_4	CdAc.	0.1	1	Powder
S_5	$CdCl_2$	0.1	1	Powder
S_6	CdAc.	0.1	1.5	Powder
S_7	$CdCl_2$	0.1	1.5	Powder
S_8	CdAc.	0.1	0	Thin film
S_9	CdAc.	0.1	1	Thin film
S_{10}	CdAc.	0.1	1.5	Thin film
S_{11}	$CdCl_2$	0.1	0	Thin

				film
S_{12}	$CdCl_2$	0.1	1	Thin film
S_{13}	$CdCl_2$	0.1	1.5	Thin film

2.2 Characterization

FTIR type (Shimadzu-8400S) was used to characterize the bonding groups of the prepared samples. The structural properties of the samples were investigated by XRD model (X'Pert Pro MPD by PANalytical Company, with CuKα radiation). The XRD patterns of thin films and powders were recorded at room temperature. The optical properties were measured by UV-Vis Spectrophotometer model (Thermospectronic heliosα V4.60). The TEM images of samples were measured by Libra 120-Carl Zeiss transmission electron microscopy.

3. Results and discussion

3.1 The FTIR spectra

FTIR spectrometer is usually used to measure the absorption of various infrared light wavelengths by material of interest. In this work it is used to examine the structure of CdS nanoparticles and the structure of PVA capped CdS nanoparticles.

Figure 2 shows the FTIR transmittance spectra of the CdS nanoparticles which prepared by using two sources. The FTIR frequencies along with the vibrational assignments for CdS nanoparticles and CdS/PVA nanocomposites are listed in Table 2. The bands at 3448.49 cm^{-1} were attributed to the O-H stretching vibration of surface hydroxyl groups involved in hydrogen bonds with water molecules. The bands at 1637.45 cm^{-1} belong to CdS nanoparticles–Cd acetate source corresponded to the O-H bending vibration of absorbed water molecules. Meanwhile, the bending vibration of water molecules appeared at 1633.59 cm^{-1} for CdS nanoparticles-$CdCl_2$. the transmittance features at 1552.59 cm^{-1} and 1402.15 cm^{-1} belong to C-C stretching and C-O unsymmetrical stretches respectively. Trace amount of SO_4 as impurity was observed at

1016.42 cm^{-1} and 1008.7 cm^{-1} for CdS nanoparticles (Cd acetate and $CdCl_2$ as sources). The vibration absorption peak of Cd-S bond was observed at 653.82 cm^{-1}, which established the generation of CdS nanoparticles [H. Wang *et al*. 2007].

Figure 3 and Table 2 shows the FTIR transmittance spectra of PVA capped CdS nanoparticles which prepared by using $CdAc_2$ and $CdCl_2$ to form CdS nanoparticles with PVA matrix. The Cd-S vibrational absorption band was observed at 653.82 cm^{-1}, which indicates formation of CdS naNOPARTICLES. However, the O-H stretching vibration band of PVA capped CdS nanoparticles became wider and weaken in intensity comparing with pure PVA and CdS. The incorporation of CdS nanoparticles has led to a small changing in the magnitude of some FTIR peaks.

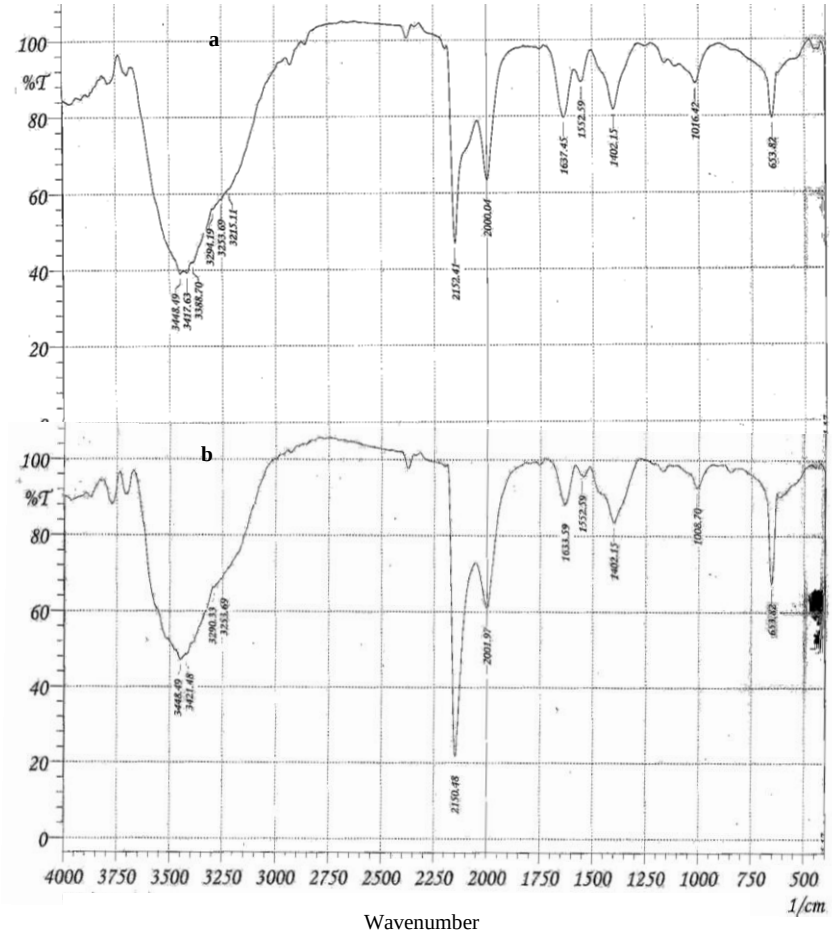

Fig.2: FTIR spectra of (a) CdS nanoparticles (CdAc2) (b) CdS nanoparticles (CdCl2).

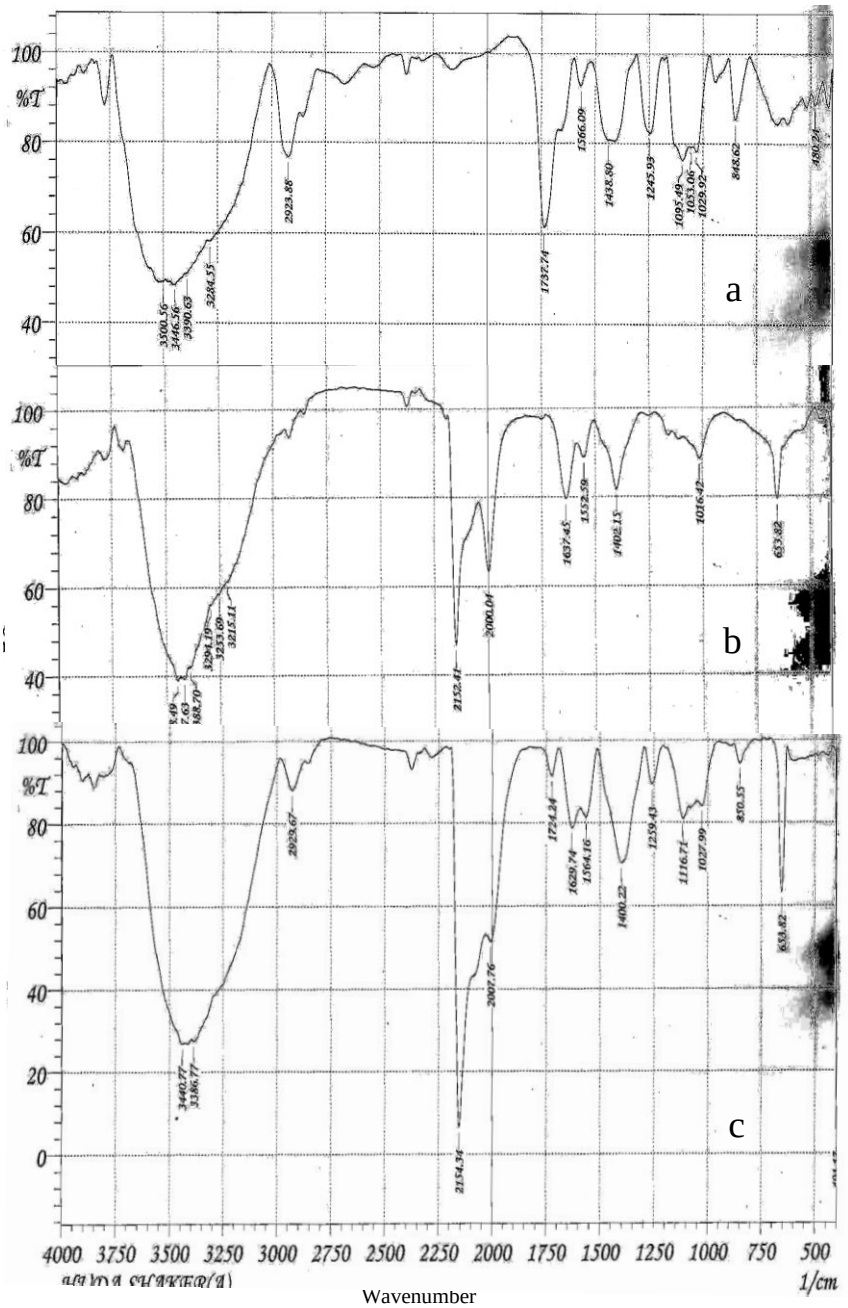

Fig.3: FTIR spectra of (a) pure PVA (b) PVA capped CdS-(1gm.) nanoparticles with $CdCl_2$ ion source (c) PVA capped CdS-(1gm.) nanoparticles with CdAc2 ion source.

Table (2): The vibration bands of FTIR for PVA capped CdS nanoparticles.

Assignments	Bond (cm^{-1})				
	PVA	**CdS (Cd ac)**	**CdS ($CdCl_2$)**	**PVA+ CdS(ac)**	**PVA+ CdS(Cl_2)**
OH stretching	3446.56 $_s$	3448.49$_s$	3448.49 s	3440.77	3448.49$_s$
C-H stretching	2923.88 2852.94	-	-	2929.67	2923.88 2852.94
C=C stretching	-	2152.41 2000.04	2150.48 2001.97	2154.34 2007.76	2146.62 2000.04
C-O stretching	1737.74$_s$	1637.45 m	1633.59 m	1724.24 1629.74	1625.88 m
C-C stretching	1566.09$_w$	1552.59 w	1552.59 w	1564.16	-
C-O stretching	1438.80$_m$	1402.15 m	1402.15 m	1400.22	1382.87
C-O stretching	1095.49 1029.92	-	1008.7	1259.43 1116.71	-
SO^-_4 as trace	-	1016.42	-	1027.99	1020.27

	848.62	-	-	850.55	848.62
Cd-S stretching	-	653.82_m	653.82	653.82	653.82

3.2 The TEM images

Figure 3 shows the TEM images of CdS/PVA nanocomposites. The TEM images showed that the CdS nanoparticles are connected with the polymer chains. Furthermore, some CdS particles have the big size indicating that it had grew outside the polymer controlling chain.

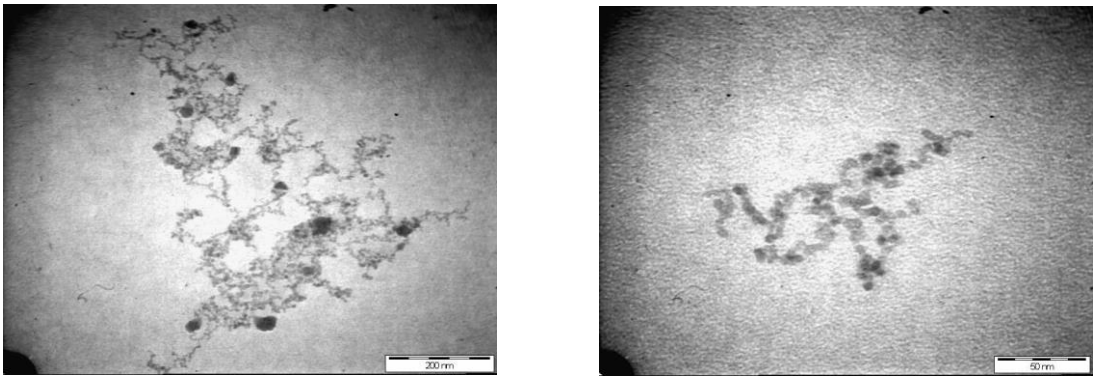

Fig.4: TEM images of a) PVA. b) CdS/PVA nanocomposites.

3.3 Structural analysis

The prepared samples were characterized by the X-ray diffraction spectra (XRD) as shown in figures 5 and 6. All the diffraction peaks were in good agreement with those of the hexagonal wurtzite structure of CdS (JCPDS 00-001-0780). It is known that the crystalline nature of PVA results from the strong intermolecular interaction between PVA chains through the intermolecular hydrogen bonding [10]. From Fig 5, after being complicated with S^{2-}, the PVA lines were hiding when Cd salt is added. It should be noted that the interactions between the PVA chains and the CdS particles has led to the decrease of intermolecular interaction of PVA chains, which had resulted in decreasing the crystalline degree of PVA.

Also, it can be seen that the XRD peaks intensity decreased with increasing the PVA ratio. The highest diffraction intensity value was corresponding to (002) plane indicated that the preferred orientation of CdS nanoparticles in this direction. The lattice constants of CdS nanoparticles in PVA calculated using the relation [B. D. Cullity 1972] :

$$\frac{1}{d^2} = \frac{4}{3}\left[\frac{h^2 + hk + k^2}{a_o^2}\right] + \frac{l^2}{c_o^2} \quad \ldots\ldots\ldots 1$$

Where h ,k and l represented the Miller's indices, a_o and c_o are the lattice parameters and d represents the inter-planar spacing d_{hkl} which was calculated for the (002) plane using the Bragg's relation [R.Maity and K.K. Chattopadhyay 2006]:

$$d_{hkl} = \frac{n\lambda}{2\sin\theta} \quad \ldots\ldots..2$$

The particle size P_S of CdS nanoparticles and CdS/PVA nanocomposites thin films were calculated using Sherrer formula [B. D. Cullity 1972]:

$$P_S = K\lambda / \beta\cos\theta \ldots\ldots\ldots\ldots 3$$

Where β is the full width at half maximum (FWHM) of the peak corrected for instrumental broadening, λ is the wavelength of the X-ray radiation (0.154 nm) and K is a constant (0.94).

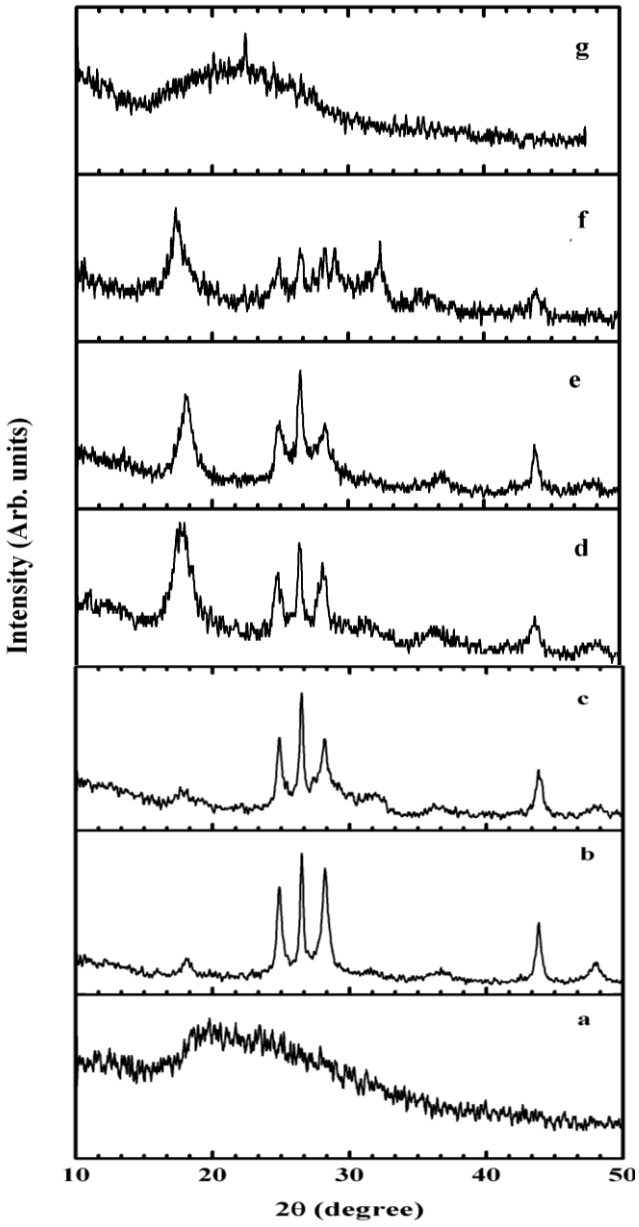

Fig.5: XRD patterns of samples: **(a) S_1, (b) S_2, (c) S_3, (d) S_4, (e) S_5, (f) S_6** and **(g) S_7**.

The strain value (ε) can be evaluated by using the following relation [N. Choudhury and B.K.Sarma 2009]

$$\xi = \frac{a_o - a}{a_o} \qquad \ldots\ldots 4$$

Where a and a_o are the lattice parameters of the thin film samples and bulk samples, respectively.

The dislocation density (δ), defined as the length of dislocation lines per unit volume

of the crystal and has been calculated by using the formula [B. D. Cullity 1972]:

$$\delta = \frac{1}{(P_s)^2} \qquad \ldots\ldots\ldots 5$$

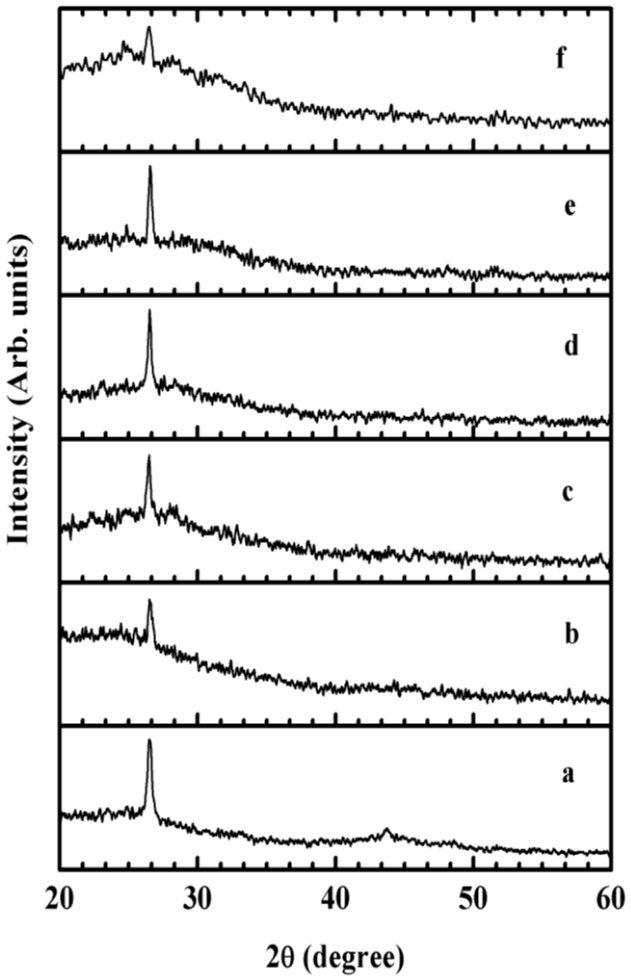

Fig.6: XRD patterns of thin films: **(a) S_8**, **(b) S_9**, **(c) S_{10}**, **(d) S_{11}**, **(e) S_{12}** and **(f) S_{13}**.

Table (3): The structural parameters for CdS powder, CdS thin films, PVA capped CdS nanoparticles and CdS/PVA nanocomposites thin films.

Sample	d_{hkl} A	Ps nm	ε %	$(lin^{-2}m^{-4})$ δ lin/m^2x10^{15}
S_1	-	-	-	-
S_2	3.36	32.0	-	-
S_3	3.36	30.0	-	-
S_4	3.35	30.8	-	-
S_5	3.36	46.0	-	-
S_6	3.36	23.0	-	-
S_7	3.35	26.0	-	-
S_8	3.36	52.0	0.29	0.37
S_9	3.36	29.7	0.51	1.10
S_{10}	3.36	41.6	0.36	0.57
S_{11}	3.36	41.6	0.36	0.57
S_{12}	3.35	29.7	0.50	1.10
S_{13}	3.36	20.0	0.72	2.20

3.4 Optical properties

The CdS thin films which prepared using CdAc2 had energy gap of 2.58 eV while the film that prepared using $CdCl_2$ had 2.66 eV. Figure 7 shows the optical absorption spectra as a function of the wavelength for PVA capped CdS nanoparticles and CdS/PVA nanocomposites thin films. All films showed a high transmission at wavelength longer than 500 nm. The values of the energy gap were calculated using the relationship [L. Brus 1984]:

$$E_g(eV) = \frac{1240}{\lambda_c(nm)} \qquad \ldots\ldots 7$$

Where λ_c represents the cut-off wavelength

From the figure 7 it can be noted that the cutting off wavelength shifts towards the red region of electromagnetic spectrum which means increasing in the optical energy gap. In nanosize materials, the expanding in energy gap happen due to the quantum confinement effect that appeared when the particles size approached to Boher radius as well as the surface state effects [L. Brus 1984].

According to the effective mass model, the energy gap of semiconductors is dependent on the particle size as showed in Burs relation [L. Brus 1984]:

$$E_{gn} = E_g + \frac{\hbar^2\pi^2}{2r^2}\left(\frac{1}{m_e^*} + \frac{1}{m_h^*}\right) - \frac{1.8e^2}{4\pi\varepsilon\varepsilon_0 r} \qquad \ldots\ldots 8$$

Where E_{gn} is an energy gap of nanoparticles, E_g the energy gap of bulk (CdS=2.42), m_e^* and m_h^* the effective mass of electron and hole, for CdS equalled 0.19me and 0.8me ,respectively, r is the radius of particle, ε is the dielectric constant (5.7) and εo is the permittivity of free space. Equation 8 has been used to calculate the values of Egn of the CdS/PVA nanocomposites thin films and are listed in Table 4.

The variations in the values of table 4 are systematic except sample S_9. There is a direct variation between Eg and Ps.

Table (4): The calculated energy gap and the particle size of CdS and CdS/PVA nanocomposites thin films

Sample	λ_c nm	E_{gn} (eV)	P_s nm
S_8	479	2.58	5.2
S_9	462	2.68	4.5
S_{10}	474	2.61	5.0
S_{11}	465	2.66	4.6
S_{12}	458	2.70	4.4
S_{13}	450	2.75	4.1

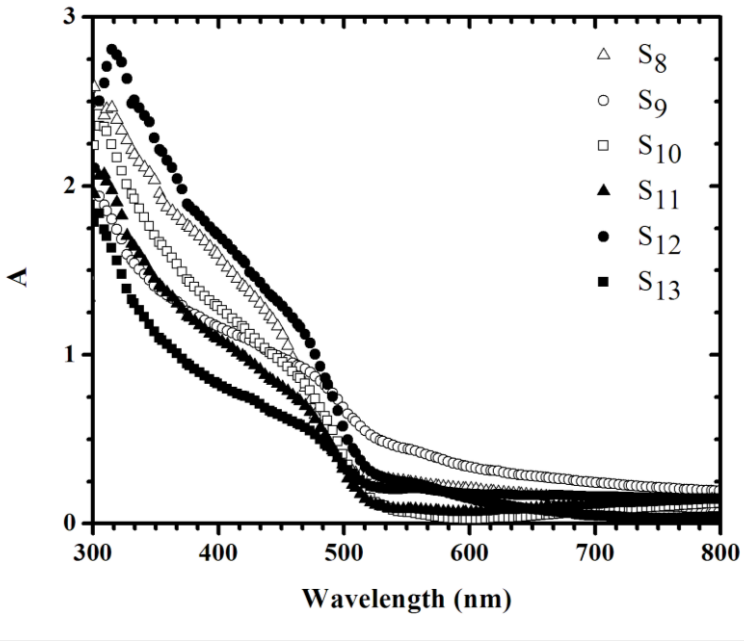

Fig.7: The optical absorption spectra of CdS and CdS/PVA nanocompsits thin films prepared using CdAs and $CdCl_2$ as source of Cd^+.

4. Conclusions

The PVA capped CdS nanoparticles and CdS/PVA nanocomposites thin films were prepared using chemical bath deposition method. The CdS nanoparticles have been successfully synthesized within PVA matrix forming PVA capped CdS nanoparticles as participation and CdS/PVA nanocomposites

thin films on glass substrates. The FTIR transmittance features were used to monitor the vibrational absorption peak of the Cd-S bond at 653.82 cm^{-1}, which indicated the formation of the PVA-capped CdS nanoparticles. The XRD patterns showed the formation of PVA capped CdS nanoparticles and the CdS/PVA nanocomposites thin films were of the hexagonal wurtzite structure. The peak's intensity of the PVA capped CdS nanopaticles decreased with increasing the PVA ratio. The particle sizes of the nanoparticles and nanocomposites thin films could be controlled in the nanometer range by adjusting the PVA concentrations and the type of Cadmium source which were coordinated in solution. From the optical absorption properties, it is found that the energy gap and the particle size of CdS/PVA nanocompsites thin films depend on the type of Cd source and the PVA concentration.

References

H.F Al-Taay *et al*. (2013)Controlling the diameter of Silicon Nanowires grown usinga tin catalyst. Materials Science in Semiconductor Processing, 16, 15-22, 2013.

M.A. Mahdi, *et al*.(2012) Structural and Optical Properties of Nanocrystalline CdS Thin Films Prepared using Microwave-Assisted Chemical Bath Deposition. Thin solid films, 520, 3477-3484, 2012.

H. Zhao, *et al.*(2001) Preparation of CdS Nanoparticles in Salt-Induced Block Copolymer Micelles. Langmuir, 17, 8428– 8433, 2001.

H.F Al-Taay *et al*.(2013) Preparation and Characterization of Silicon Nanowires Catalyzed by Aluminum. Physica E, 48, 21-28, 2013.

M.A. Mahdi, *et al.* (2012)Growth and Characterization of $Zn_xCd_{1-x}S$ nanoflowers by microwave-assisted chemical bath deposition, J. Alloys Compd. 541, 227-233, 2012.

J. Kuljanin, *et al*. (2006) Synthesis and characterization of nanocomposite of polyvinyl alcohol and lead sulfide nanoparticles. Materials Chemistry and Physics, 95, 67-71, 2006.

S.H. Liu, *et al*. Synthesis and Characterization of Ag_2S Nanocrystals in Hyperbranched Polyurethane at Room Temperature. J. Solid State Chem., 168, 259-262, 2002.

I.S. Elashamawi, *et al*. (2009)Optimization and spectroscopic studies of CdS/PVA nanocomposites. Materials Chemistry and Physics., 115, 132-135, 2009 .

J. D. Patela, *et al.* (2009) Synthesis of PbS/poly (vinyl-pyrrolidone) nanocomposite. Materials Research Bulletin, 44(8), 1647-1651, 2009 .

M. Pattabi, et al. (2007)Photoluminescence study of PVP capped CdS nanoparticles embedded in PVA matrix. Materials Research Bulletin, 42, 828–835, 2007.

W. Qingqing, *et al.* (2005) Solvothermal synthesis and characterization of uniform CdS nanowires in high yield. Jr of Sold. St. Chem., 178(9), 2680-2685,2005 .

R.Maity and K.K. (2006) Chatto-padhyay. Synthesis and optical characterization of CdS nanowires by chemical process. J. Nanopart. Res., 8, 125–130, 2006.

Y.C. Zhang, *et al*. (2007) Solvothermal synthesis of hexagonal CdS nanostructures from a single-source molecular precursor. J. Alloys Compd., 437, 47–52, 2007.

H. Wang , *et al*.(2007) Synthesis and characterization of CdS/PVA nanocomposite films. Applied Surface Science ,253, 8495–8499, 2007 .

B. D. Cullity, (1972)Elements of X-Ray Diffraction. Addison-Wesley, Reading, MA, 1972.

L. Brus,(1984) Electron–electron and electron-hole interactions in small semiconductor crystallites: The size dependence of the lowest excited electronic state. J. Phys. Chem., 80, 4403, 1984.

N. Choudhury and B.K.Sarma, (2009)"Bull. Mater. Sci.", 32 , 43–47, 2009.

الخصائص التركيبية والبصرية للاغشية الرقيقة للتركيبات النانوية CdS/PVA

فرقان عبدالله قاسم

قسم الفيزياء – كلية العلوم – جامعة البصرة

furqan_kasim@yahoo.com

الملخص:

تحضر الاغشية الرقيقة للتركيبات النانوية لـ CdS/PVA بطريقة الترسيب الكيميائي على قواعد زجاجية بدرجة حرارة 75 سيليزية. اذ يستخدم خلات الكادميوم وكلوريد الكادميوم كمصدر لايونات الكادميوم بينما تستخدم الثايوريا كمصدر لايونات الكبريت مع اضافة تراكيز مختلفة من البوليمر (بولي كحول الفاينيل). درست الخصائص التركيبية للعينات المحضرة باستخدام جهاز حيود الاشعة السينية XRD فتؤثر نسب البوليمر على البارامترات التركيبية (ثابت الشبيكة، ثابت المطاوعة وكثافة التشويه). تم تشخيص وتحديد الاواصر باستخدام جهاز الاشعة تحت الحمراء FTIR. واخذت صور الماسح الالكتروني لاحد العينات لمعرفة التاصر للتركيبات النانوية CdS/PVA. درس طيف الامتصاص البصري لاغشية التركيبات النانوية CdS/PVA وتم حساب قيم فجوة الطاقة. تم حساب حجم الجسيمات للجسيمات النانوية لمركب كبريتيد الكادميوم وللاغشية الرقيقة للتركيبات النانوية لمركب كبريتيد الكادميوم من منحنيات حيود الاشعة السينية وفجوة الطاقة البصرية.